Coherent population trapping in ruby crystal at room temperature

Roman Kolesov
Department of Physics and Institute for Quantum Studies,
Texas A&M University,
College Station, Texas 77843-4242

(Dated: February 2, 2008)

Observation of coherent population trapping (CPT) at ground-state Zeeman sublevels of Cr^{3+}-ion in ruby is reported. The experiments are performed at room temperature by using both nanosecond optical pulses and nanosecond trains of ultrashort pulses. In both cases sharp drops in the resonantly induced fluorescence are detected as the external magnetic field is varied. Theoretical analysis of CPT in a transient regime due to pulsed action of optical pulses is presented.

arXiv:physics/0505051v1 [physics.optics] 6 May 2005

In last few decades very much attention has been paid to studying optical interference phenomena originating from the atomic coherence excited by laser light while interacting with multi-level atomic media. These phenomena include coherent population trapping (CPT) [1], electromagnetically induced transparency (EIT) [2], lasing without population inversion (LWI) [3], slow light [4], and many others. The interest to this field arises from a number of potential applications of these phenomena. Among them are metrology, quantum information storage and processing, ultra-sensitive magnetometry, development of lasers in vacuum ultraviolet (VUV), X-ray, and γ-ray ranges, etc. However, CPT and related phenomena are mostly being studied in gaseous media while for practical purposes solid-state materials are preferable. The advantages of solids are high atomic density, absence of atomic diffusion, compactness, and robustness. At the same time, decoherence processes in solid media are severe. Nevertheless, several demonstrations of EIT [5, 6], slow light [5], and non-degenerate four-wave mixing [7] in solids have been reported by several groups. However, all those works were performed at temperatures close to the liquid helium one. This fact, in turn, makes real solid-state applications of the above phenomena questionable.

In this Letter I report the first, to my knowledge, experimental observation of CPT resonances in crystalline solid at room temperature. Prior to that, I have to discuss some general issues in order to identify the class of solid-state materials in which the phenomena of EIT/CPT can be observed at room temperature. I will consider only optical crystals doped with either rare-earth or transition metal ions possessing discrete electronic states in the bandgap of the host material. The electronic transitions between those states, both optical and Zeeman and/or hyperfine, can be very narrow even at room temperature. The class of so-called S-state ions doped into wide-bandgap optical crystals is of particular interest. It includes Cr^{3+}, Eu^{2+}, Fe^{3+}, Mn^{4+}, Gd^{3+}, and several others. The most important feature of these ions is that, when incorporated into a crystal, their first excited electronic state lies several thousands cm^{-1} above the ground one. Consequently, the strongest relaxation process between the ground-state Zeeman or hyperfine sublevels, owing to resonant inelastic scattering of phonons at low-energy electronic transition (Orbach relaxation, [8]) is suppressed. As a result, the decoherence rate at the transitions between Zeeman/hyperfine sublevels can be as low as a few MHz even at room temperature. This fact is confirmed by a vast number of electron paramagnetic resonance (EPR) measurements in which the ions mentioned above serve as paramagnetic probes. Some of them, namely, Cr^{3+}, Eu^{2+}, and Gd^{3+}, offer very favorable optical properties as well. In the following discussion, the case of ruby, i.e. $Cr^{3+} : Al_2O_3$, is considered.

Another important feature of doped solids is that the population decay from the excited electronic state is much slower than decoherence at Zeeman/hyperfine transition. This is exactly opposite to the case of alkali-metal vapors in which most of experimental work on EIT/CPT is being performed. Therefore, one cannot expect to populate the coherent superposition of ground-state sublevels, which does not interact with the laser field under the conditions of CPT (so-called, "dark" state), by decay of the excited optical level, as is the case in the alkali-metal experiments. The only way of exciting ground-state coherence in that situation is to remove as much population as possible from the "bright" state (the coherent superposition of sublevels orthogonal to the "dark" one) by transferring it to the upper optical level. This should be done faster than the coherence decays, i.e. laser excitation has to be pulsed.

Let us consider the following theoretical model. A three-level medium is illuminated with a resonant laser pulse interacting with both $1 \leftrightarrow 3$ and $2 \leftrightarrow 3$ optical transitions (see inset of Fig.1). In the rest of the paper we will be interested in the amount of population transferred into level 3 by a laser pulse or pulse train as a function of the energy separation between ground-state Zeeman sublevels 1 and 2 which can be varied by means of external magnetic field. The following notations are introduced: Γ is the homogeneous halfwidth of optical transitions, γ is the Zeeman decoherence rate, Ω is the laser field time-dependent Rabi frequency (dipole

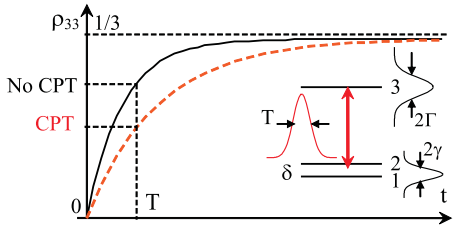

FIG. 1: Temporal evolution of the upper optical state population under pulsed excitation. The inset shows the model of a three-level atomic medium interacting with light pulse.

matrix elements of both optical transitions are assumed equal). The initial populations of the two ground-state sublevels are $\rho_{11} = \rho_{22} = 1/2$, $\rho_{33} = 0$. Assume also, that the pulse duration is longer than Γ^{-1}, γ^{-1}. This assumption somewhat contradicts the last statement in the previous paragraph, but it is relevant under the experimental conditions described below. Algebraically solving the density matrix equations for all the coherences, one comes to the following linear equation for the upper state population:

$$\frac{\rho_{33}}{dt} = P\left(1 - \frac{P\left(P+\gamma\right)}{\delta^2 + \left(P+\gamma\right)^2}\right)\left(1 - 3\rho_{33}\right), \qquad (1)$$

where $P = 2\Omega^2/\Gamma$ and δ is the frequency separation between the ground-state sublevels. The second term in brackets represents the effect of Zeeman coherence on the rate at which level 3 is populated. Laser pulse starts acting on the medium at $t = 0$. As $t \to \infty$, all three levels become equally populated, as expected. However, if at some instant T the laser pulse is shut off, the final population of level 3 is smaller for $\delta = 0$ than it is for $\delta \neq 0$ because of its lower growth rate as illustrated in Fig.1. The width of this transient CPT resonance is determined by $P + \gamma$, i.e. by Zeeman decoherence rate and power broadening.

Similar effects can be observed under the illumination of the medium with a short (nanosecond) train of ultrashort (picosecond) pulses. In addition to CPT resonance at zero magnetic field, one should expect drops in the upper state population as the Zeeman sublevel separation becomes equal to the multiple of the pulse repetition rate in the train [9]. It worths mentioning that transient coherent effects in ruby crystal at room temperature were first studied in 1974 [10]. In that work precessing magnetization was induced by a train of ultrashort pulses. Significant enhancement in magnetization was observed as the splitting between Zeeman sublevels of Cr^{3+}-ion became multiple of the pulse repetiotion rate. However, no effect of Zeeman coherence on the absorptive properties of the crystal was studied.

To understand how the above theoretical description applies to ruby, let us consider the energy levels of Cr^{3+} in that crystal (see Fig.2). Its ground state is described

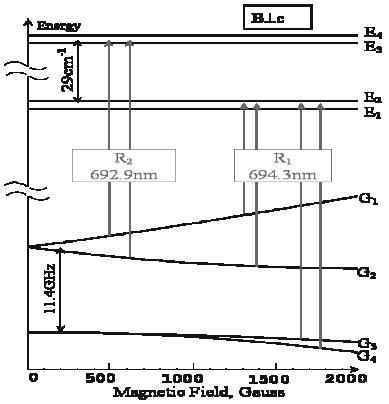

FIG. 2: Energy levels of Cr^{3+}-ion. Optical transitions allowed for σ-polarization in $\mathbf{B} \perp c$ geometry are indicated.

by the following spin Hamiltonian:

$$H = g_{||}B_{||}S_z + g_{\perp}\mathbf{B}_{\perp}\mathbf{S}_{\perp} + D\left(S_z^2 - S\left(S+1\right)/3\right), \quad (2)$$

where $g_{||} = 1.982$ and $g_{\perp} = 1.987$ are the ground-state g-factors in the directions parallel and perpendicular to the crystal c-axis respectively, $B_{||}$ and $\mathbf{B}_{\perp}$ are the corresponding magnetic field components, $2D = -11.47\ GHz$ is the zero-field splitting of the ground state, and $S = 3/2$ is the spin of Cr^{3+}. The excited optical state is split into two spin-doublets separated by 29 cm^{-1} giving rise to R_1 (694.3 nm) and R_2 (692.9 nm) optical lines of ruby. The width of both optical transitions is 11 cm^{-1} while the oscillator strength is 7.5×10^{-7}.

The situation when $\mathbf{B} \perp c$-axis is of particular interest. The selection rules for $\sigma^{\pm}$-polarizations of light propagating along the c-axis are summarized in Tables I and II [11]. The matrix elements are normalized so that the sum of their squares for each of the $\sigma^{\pm}$-polarizations is unity. One can easily see that there are a number of Raman processes connecting levels G_1 and G_2 and G_3 and G_4. Since the optical linewidth is greater than the separation between the ground-state Zeeman sublevels, all Λ-systems will give their contributions to the Zeeman coherence excitation. Therefore, if one uses a linearly polarized laser light, the net contribution of all Raman processes to the coherence excitation at either $G_1 \leftrightarrow G_2$ or $G_3 \leftrightarrow G_4$ transition is exactly zero. For example, at R_2-line the coherence between levels G_1 and G_2 due to Raman process going though E_3 for σ^+-polarization is exactly compensated by the one going though E_4 for σ^--polarization. The situation is the same for R_1-line. However, there is no such difficulty for circularly polarized light.

The experiments were performed on a $3 \times 3 \times 5\ mm^3$ dilute ruby crystal (0.002% of Cr^{3+}) with c-axis being perpendicular to one of $3 \times 5\ mm^2$ sides (Scientific Materials Corp.) A homemade tunable Ti:Sapphire laser pumped by the doubled $Nd:YLF$ pulsed laser (Photonics Industries, model GM-30) could operate both in a long

State	G_1	G_2	G_3	G_4
E_1	± 0.25	0.25	-0.31	± 0.31
E_2	0.25	± 0.25	± 0.31	-0.31

TABLE I: Selection rules for σ^+ (upper sign) and σ^- (lower sign) polarizations interacting with R_1-line.

State	G_1		G_2	
	σ^+	σ^-	σ^+	σ^-
E_3	0.43	-0.07	-0.43	-0.07
E_4	-0.07	-0.43	0.07	-0.43

TABLE II: Selection rules for $\sigma^\pm$ polarizations interacting with R_2-line. Transitions from the lower ground-state doublet to levels E_3 and E_4 are forbidden.

pulse regime (pulse duration $\approx 30\ ns$ FWHM) and in a mode-locked regime delivering $\approx 30\ ns$ pulse trains with repetition rate $\approx 260\ MHz$. The laser was mode-locked by using a cryptocyanine saturable absorber dissolved in ethanol. The typical output energy per pulse or per train was several tenths of a mJ at a $100\ Hz$ repetition rate. The laser polarization was linear. The typical shapes of pulses in both regimes are shown on the insets of Figs.3 and 4. The shape of the pulse train was taken with a $350\ ps$-risetime photodiode and a $500\ MHz$-bandwidth oscilloscope. The duration of each individual pulse in the train was not measured. The crystal was placed into a varying magnetic field with $\mathbf{B} \perp c$-axis and illuminated by laser pulses sent through a $\lambda/4$-plate and focused by an $f = 10\ cm$ lens. Presumably, the laser spot diameter at the sample was $\sim 100\ \mu m$. The fluorescence was detected as a function of slowly varying periodic magnetic field. The sweeping frequency of the magnetic field was $0.17\ Hz$.

The experimental results for the case of long pulse excitation for both R_1 and R_2 lines are shown in Fig.3. The spectra were averaged over several hundreds of magnetic field sweeps. In the case of R_1-line, there are two features present in the spectrum: the broad one with the plateau on the bottom and a sharp one of much smaller amplitude. The smaller one corresponds to less than 0.5% decrease in the fluorescence amplitude and has a width of 18 G. It corresponds to CPT resonance due to $G_1 \leftrightarrow E_1, E_2 \leftrightarrow G_2$ Λ-system, thus its width in terms of frequency units is $\approx 100\ MHz$ since g-factor for $G_1 \leftrightarrow G_2$ transition is ≈ 4. The broad drop in fluorescence signal has an amplitude $\approx 7 - 8\%$. Its FWHM is close to $\approx 950\ G$. The presence of plateau at the bottom of that feature indicates that this is a CPT resonance in the $G_3 \leftrightarrow E_1, E_2 \leftrightarrow G_4$ Λ-system with levels G_3 and G_4 being split very slowly as the magnetic field increases. Its width recalculated into frequency domain is $\approx 40 - 50\ MHz$, i.e. this CPT resonance is, in fact, much sharper than the one discussed above. The possible explanation for this fact is as follows. The main contribution to the EPR linewidth of Cr^{3+} in ruby is known to originate from magnetic dipole-dipole hyperfine interaction with neighboring ^{27}Al nuclei [12]. Thus, the magnetic-allowed Zeeman transition $G_1 \leftrightarrow G_2$ should be broadened much stronger than the magnetic-forbidden $G_3 \leftrightarrow G_4$. This also explains more than an order of magnitude difference in the amplitudes of those two CPT resonances, since in Λ-system with longer-lived Zeeman coherence CPT should be more pronounced.

For the R_2-line only one CPT resonance, represented by a sharp feature at the bottom of a smooth background, is observed. It has the width of 18 G, i.e. the same as the one observed at R_1-line, thus it corresponds to $G_1 \leftrightarrow E_3, E_4 \leftrightarrow G_2$ Λ-system. The decrease in the fluorescence is $3-4\%$ at the center of the resonance. The fact that this resonance is much stronger is easily understandable, since 1) there is no background fluorescence excited from the other pair of levels, G_3 and G_4, and 2) the transitions $G_1, G_2 \leftrightarrow E_3, E_4$ are 3 times stronger than $G_1, G_2 \leftrightarrow E_1, E_2$. The smooth background originates, probably, from level mixing in high magnetic fields and consequent change in the optical selection rules. That was confirmed by removing the $\lambda/4$-plate, i.e. by making laser light linearly polarized. Under this condition all three CPT resonances, discussed above, disappeared, as they were supposed to, while the smooth feature in question remained.

The results for trains of ultrashort pulses are shown in Fig.4. In the spectrum obtained for R_1-line additional resonances appear in pairs. They are not equidistant because of nonlinear dependence of the levels G_3 and G_4 separation on the magnetic field strength. However, if recalculated into frequency domain, their positions exactly correspond to the harmonics of laser repetition rate ($260\ MHz$). The first three of them are shown on the inset of Fig.4a. Their widths (FWHM) are in the range $35-38\ MHz$ and their positions, according to the fit, are $265\ MHz$, $533\ MHz$, and $804\ MHz$. The widths are in rather good agreement with the result obtained for the $G_3 \leftrightarrow G_4$ transition in a long pulse regime. It was not possible to observe multiple CPT resonances corresponding to $G_1 \leftrightarrow E_3, E_4 \leftrightarrow G_2$ Λ-system with appreciable signal-to-noise ratio due to very small amplitude of the CPT effect ($< 0.5\%$) and rather unstable operation of laser in a mode-locked regime. However, the signature of these resonances is the increased quasi-noise at the bottom of the broad feature.

For R_2-line almost 30 CPT resonances are indicated. In order to improve the signal-to-noise ratio, the original spectrum was flipped with respect to the zero magnetic field and the two sets of data were combined together. That explains the fact that the plot shown in Fig.4b is completely symmetric. The magnetic field separation be-

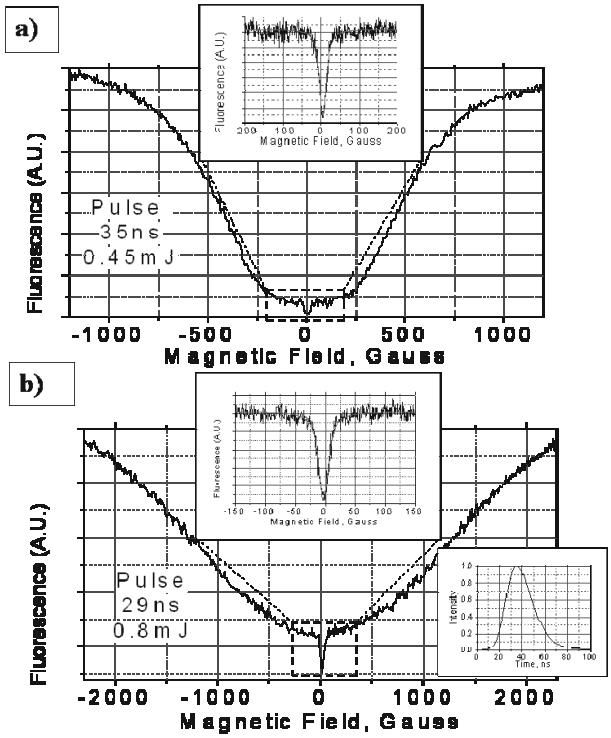

FIG. 3: CPT resonances in zero magnetic field: a) trace for R_1-line and b) trace for R_2-line. Narrow peaks are shown in detail on insets. See text for details.

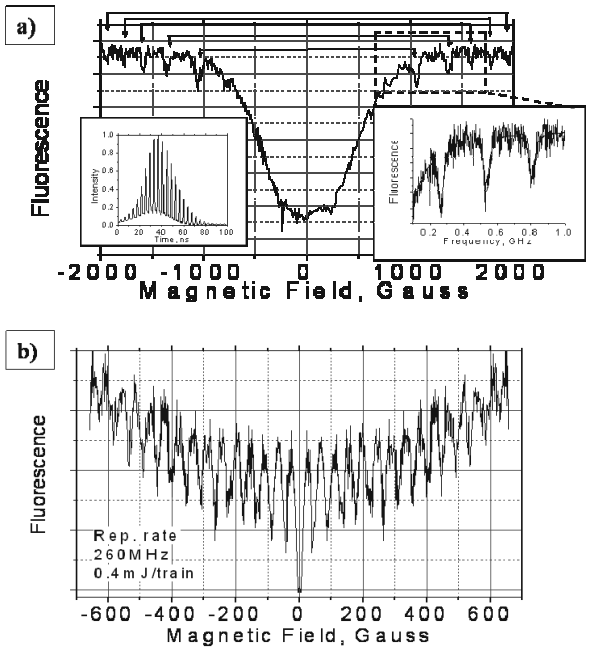

FIG. 4: CPT resonances with mode-locked laser: a) trace for R_1-line and b) trace for R_2-line. See text for details.

tween each pair of resonances is $\approx 45\ G$. This value corresponds to 252 MHz of frequency separation which is somewhat close to 260 MHz of laser repetition rate. Due to rather poor signal-to-noise ratio and rater low spectral resolution it is not possible to determine the linewidth of resonances exactly, but it seems to correspond rather well to the value of 18 G obtained in a long pulse regime.

In summary, the first observation of CPT in a crystal at room temperature is reported. Possible applications of the reported phenomena include room-temperature all-optical analogue of EPR spectroscopy in low magnetic fields, suppression of excited state absorption in laser crystals [13], alternative technique of mode-locking in lasers [14], etc.

The author is grateful to F.Vagizov, P.Hemmer, Y.Rostovtsev, E.Kuznetsova, and O.Kocharovskaya, for stimulating discussions and to S.Lissotchenko for technical assistance. The work was supported by NSF and AFOSR.

[1] E. Arimondo, in *Progress in Optics*, edited by E. Wolf (Elsevier, Amsterdam, 1996), Vol. 35, pp. 257-354
[2] J.P. Marangos, J. Mod. Opt. **45**, 471 (1998); S.E.Harris, Phys. Today **50**, 36 (1997)
[3] J. Mompart and R. Corbalan, J. Opt. B: Quantum Semiclassical Opt. **2**, R7 (2000)
[4] A.B. Matsko et al., Adv. At., Mol., Opt. Phys. **46** 191 (2001)
[5] A.V. Turukhin et al., Phys. Rev. Lett. **88**, art. no. 023602 (2002)
[6] Y. Zhao, C.K. Wu, B.S. Ham, M.K. Kim, and E. Awad, Phys. Rev. Lett. **79** 641 (1997); C.J. Wei and N.B. Manson, Phys. Rev. A **60** 2540 (1999); P.R. Hemmer, A.V. Turukhin, M.S. Shahriar, and J.A. Musser, Opt. Lett. **26** 361 (2001); M. Phillips and H.L. Wang, Phys. Rev. Lett. **89** art. no. 186401 (2002); G.B. Serapiglia, E. Paspalakis, C. Sirtori, K.L. Vodopyanov, and C.C. Phillips, Phys. Rev. Lett. **84** 1019 (2000)
[7] J.Q. Liang, M. Katsuragava, F.L. Kien, and K. Hakuta, Phys. Rev. Lett. **85** 2474 (2000)
[8] R. Orbach, Proc. Roy. Soc. (London) **A264** 458 (1961)
[9] O.A. Kocharovskaya and Ya.I. Khanin, Zh. Eksp. Teor. Fiz. **90** 1610 (1986) [Sov. Phys. JETP **63** 945 (1986)]; V.A. Sautenkov et al., Phys. Rev. A, to be published
[10] Y. Fukuda, Y. Takagi, and T. Hashi, Phys. Lett. **48A** 183 (1974)
[11] S. Sugano and Y. Tanabe, J. Phys. Soc. Jpn. **13** 880 (1958); M.O. Schweika-Kresimon, J. Gutschank, and D. Suter, Phys. Rev. A **66** art. no. 043816 (2002)
[12] N. Laurance, E.C. McIrvine, and J. Lambe, J. Phys. Chem. Solids, **23** 515 (1962); R.F. Wenzel and Y.W. Kim, Phys. Rev. **140** A1592 (1965)
[13] E. Kuznetsova, R. Kolesov, and O. Kocharovskaya, Phys. Rev. A **70** art. no. 043801 (2004); R. Kolesov, E. Kuznetsova, and O. Kocharovskaya, *ibid.* to be published
[14] O.A. Kocharovskaya, Ya.I. Khanin, and V.B. Tsaregradskii, Kvantovaya Elektron. **12** 1227 (1985) [Sov. J. Quantum Electron. **15** 810 (1985)]